Sixth International Symposium on Marine Propulsors
smp'19, Rome, Italy, May 2019

Tip vortex cavitation inception estimation at an industrial level

Urban Svennberg [1], Daniel Ahl[1] and Abolfazl Asnaghi [2]

[1] Kongsberg Hydrodynamic Research Centre, Kongsberg Maritime Sweden AB, Kristinehamn, Sweden
[2]Department of Mechanics and Maritime Sciences, Chalmers University of Technology, Gothenburg, Sweden

ABSTRACT

The demand for silent operation of propellers is increasing at the same time as higher efficiency is desired which are contradicting requirements for a propeller design. Cavitation is an important source for noise and the tip vortex cavitation is often the first type of cavitation to occur on a propeller. A method for tip vortex cavitation inception estimation at an industrial level has, therefore, been developed. It is based on sliding mesh simulation with oblique inflow to capture the tangential wake and using source terms to mimic the axial wake. It is using the dynamic Smagorinsky LES model to capture the development of the tip vortex. The method uses a lower mesh resolution than what is needed to capture the lowest pressure in the tip vortex to make it feasible for industrial use. This reduces the time consumption but increases the uncertainty and means that we have an engineering method which is not fully satisfactory from the scientific point of view. However, in an engineering context where the final propeller design is verified by model scale experiments, the increased uncertainty due to lower resolution can be handled in an acceptable way.

Keywords

Tip vortex, cavitation inception, CFD.

1 INTRODUCTION

The demand for silent operation of propellers is increasing at the same time as higher efficiency is desired. Cavitation is the most pronounced noise source for a propeller (Kuiper 1981). The ship speed where the propeller starts to generate cavitation is called the cavitation inception speed (CIS). Therefore, the CIS is a threshold where the propeller becomes considerably noisier. The owners of navy ships, cruise ships, yachts, and research vessels often include a minimum requirement on the CIS in design contracts for ships and propellers. At the same time, they want to have the most efficient propeller. Increasing the efficiency normally reduces the CIS and vice versa. Therefore, it is important to get a good estimate of the cavitation inception speed during the design of a propeller to find the most efficient propeller that reaches the desired CIS.

The tip vortex cavitation is often the first cavitation to occur, which then calls for an accurate estimation of its inception. The tip vortex has a simple explanation. A lifting surface like a wing or propeller blade have higher pressure on one side than the other and the fluid, air or water, flows from the high pressure side over the tip to the low pressure side. This overflow generates a rotation over the tip and rolls up in a vortex downstream. Even though, the basic explanation is simple it results in a very complex three dimensional flow structure and its behaviour is dependent on very small structures. Cavitation and cavitation inception add even more complexity. This type of flow field has been of scientific interest both experimentally and numerically for many years, (Arndt et al 1991), (Mains and Arndt 1997), and the computational capacity has increased to a level where detailed numerical analysis is possible, (Asnaghi et al 2017a), (Asnaghi et al 2017b), (Asnaghi et al 2018a), (Hsiao and Chahine 2004) and (Windt and Bosschers 2015). Tip vortex CIS has also been of great interest for propeller manufacturers but with a normally short time frame for a commercial propeller design, it has not been possible to do a detailed numerical analysis. The design process has instead been dependent on experience, rules of thumb, simpler numerical analysis of the propeller load and model testing to determine the width and the depth of the cavitation bucket, see Figure 1.

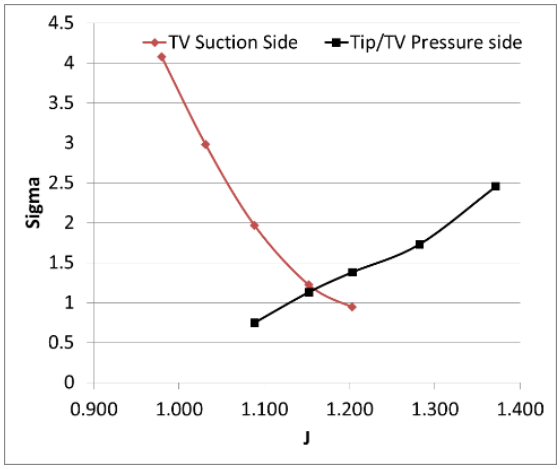

Figure 1: Example of cavitation inception bucket from the CFD method.

The location of the lowest inception point in it is of special interest. For conditions with high load on the propeller there is a strong suction side tip vortex and if the load is lowered the strength of this vortex will be reduced. But if

the load is reduced too much, a pressure side tip vortex will be created instead and it will become stronger the lower the load becomes. The propeller should be designed so that the point of normal operation is located where the inception curves for the suction side and pressure side tip vortices cross each other.

2 NUMERICAL METHOD

The method is based on a propeller with a simplified hub and shaft inside a rotating cylindrical domain inside a larger brick shaped stationary domain. The interaction between the cylinder and the outer domain is through a sliding mesh interface. The inflow to the domain is at an angle compared to the shaft to mimic a tangential wake component. The axial wake component is represented using body forces in the domain. The cavitation inception estimation is done using the pressure from a incompressible transient simulation without cavitation modelling. More details are given in the sub sections below.

2.1 Turbulence

To model the flow field by using LES approach, the low pass filtered equations of mass and momentum are employed,

$$\frac{\partial \rho}{\partial t} + \frac{\partial (\rho \bar{u}_i)}{\partial x_i} = 0\,, \tag{1}$$

$$\frac{\partial (\rho \bar{u}_i)}{\partial t} + \frac{\partial \left(\rho \bar{u}_i \bar{u}_j\right)}{\partial x_j} = \frac{\partial \bar{p}}{\partial x_i} + \frac{\partial \left(2\mu \bar{S}_{ij} - \bar{B}_{ij}\right)}{\partial x_j} + \rho g_i\,, \tag{2}$$

where ρ is the constant density of water, the over bar denotes low pass filtered quantities,

$$B_{ij} = \rho\left(\overline{u_i u_j} - \bar{u}_i \bar{u}_j\right) \tag{3}$$

is the subgrid stress tensor and g_i is external forces, for example gravitation. The strain rate tensor, $\bar{S}_{ij}$, is the symmetric part of the velocity gradient,

$$\bar{S}_{ij} = \frac{1}{2}\left(\frac{\partial \bar{u}_i}{\partial x_j} + \frac{\partial \bar{u}_j}{\partial x_i}\right). \tag{4}$$

The subgrid stress tensor is approximated using the Dynamic Smagorinsky subgrid model available in STAR-CCM+.

2.2 Geometrical Setup

Most of the propellers of interest here are used on open shafts under the hull. This means that the propeller is operating in an area with a small axial wake but with an oblique inflow. This is due to that the propeller shaft has to end inside the ship while the flow is tangential to the hull surface.

The geometrical setup is the propeller blades mounted on a simplified hub and shaft. The hub and shaft is a cylinder with elliptical ends where the user can define the upstream and downstream lengths of the shaft and the ratio for the elliptical ends. This shaft is then placed in a cylinder which is connected to an outer box through sliding mesh, see Figure 2. The size of the cylinder and the box are determined by the length of the shaft and the diameter of the propeller. The shaft inclination is decided by the angle of the inflow with more than one side of the box defined as inlet and outlet respectively resulting in an oblique flow through the domain.

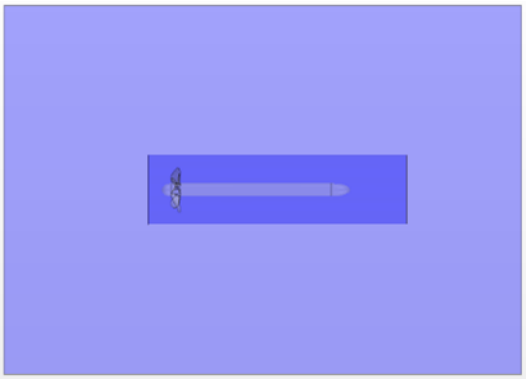

Figure 2: Example of the computational domain.

2.3 Computational Mesh

The outer box is meshed using STAR-CCM+ trimmer mesh which essentially is a Cartesian mesh with local refinement by splitting cells combined with a surface following mesh with some multi-face, cut hexahedral, cells to connect the surface mesh to the Cartesian mesh. The inner cylinder is meshed using polyhedral cells with prismatic layers on the propeller and shaft. This mesh contains about 8 million cells and result in a wall y^+ value in the range 30-60.

The computational mesh is refined around the tip and tip vortex for one blade using an industrial realistic mesh refinement, which adds another 8 million cells and results in a $y^+<1$ around the tip of the blade where the tip vortex is originating. However, this resolution is not sufficient to accurately capture the lowest pressure in the tip vortex, (Asnaghi et al 2017a). This lower resolution makes it possible to use the method in the time frame of a propeller design with moderate computational resources but it increases the uncertainty and gives over prediction of the pressure in the vortex core. This means that we have an engineering method which is not fully satisfactory from the scientific point of view. However, in an engineering context where the final propeller design is verified by model scale experiments, the uncertainty and over prediction of the pressure can be handled in an acceptable way. Furthermore, the systematic over prediction of the pressure becomes less problematic when the method primarily is used for comparison of different designs.

The simulations are still time consuming but can be done in a considerably shorter time frame than the production of a model propeller and carrying out the model test. This gives the propeller designer the opportunity to do simulations for a number of designs and have a better propeller for the validation in model tests which reduces the number of model tests needed to find a good design for challenging projects.

2.4 Cavitation Inception Criteria

The tip vortex cavitation inception process is very complex. The flow structures in the tip vortex are complex with vortices from the wake of the blade rolling up into the

tip vortex. This results in a wide range of length scales in the flow calling for a very small cell size to capture the accurate pressure distribution in the vortex, (Asnaghi et al 2017a) and (Asnaghi et al 2017b). Cavitation inception is also a complex process not only dependent on the pressure. The size and amount of cavitation nuclei, often small bubbles of gas, in the water and how these are entered into the core of the vortex can also have a large influence on the inception pressure, (Pennings et al. 2015). For more details and further references about cavitation inception see (Asnaghi et al 2018a), and (Asnaghi et al 2018b). This results in an under prediction of the CIS if a simple pressure criterion is used in a well resolved simulation, an observation that can be found in other publications as well, (Hsiao and Chahine 2005).

The cavitation number, σ, is defined as:

$$\sigma = \frac{P - P_v}{0.5\rho V_A^2} \tag{5}$$

where P is the static pressure, P_v is the vaporization pressure, ρ is the density and V_A is the free stream velocity in the simulations. Cavitation inception is assumed to occur when the local pressure is equal to P_v and the question is then at what σ is the local pressure p in the tip vortex equal to P_v. After some analysis it can be found that the inception σ can be written as:

$$\sigma_i = -\frac{p}{0.5\rho V_A^2} = -C_p \tag{6}$$

which results in an unique value for σ_i in each cell in the computational domain at each time step.

The advance number, J used in the cavitation inception diagrams is defined as:

$$J = \frac{V_A}{nD} \tag{7}$$

where n is the rate of revolution for the propeller and D is the diameter of the propeller.

The cavitation inception method used for the first computational example below is based on the pressure from a transient simulation without cavitation modelling. The highest σ_i in the relevant area of the simulation domain for each time step is stored. The highest of these stored time step σ_i for one revolution is then used as the inception σ. This method is very sensitive to numerical oscillations in the solution and the difference from geometrical changes when comparing propellers could be hidden in differences in numerical noise. Therefore, an improved model has been used for the second computational example.

The cavitation inception method used in the second example below is also based on the pressure from a transient simulation without cavitation modelling but uses a volume criterion. An iso-surface of pressure is constructed in the flow field and the volume enclosed by this surface is computed. The lowest pressure that can be set for the iso-surface, which results in a volume larger than a predefined value, is found for each time step and σ_i is calculated using this pressure and stored for each time step. The highest of these stored σ_i for one revolution is then used as the inception σ. The predefined volume can be taken as the volume a cavitation bubble needs to have to be observed in a cavitation experiment or it can be used to fine tune an engineering method. Numerical pressure spikes often come from single cells of low quality and by this method these are filtered out to a large extent when the volume for the volume criteria is larger than the cells in the part of the domain that is analyzed.

2.5 Wake Approximation

In some cases with open shafts there is a very small axial wake component and in these cases it can be neglected and it is sufficient to have the tangential wake component which is mimicked using an oblique inflow. For applications which have an axial wake there is a need to represent it to get accurate results. Here, the axial wake component is represented by applying body forces to the momentum equations, i.e. give g_i in Equation (2) a value. The body forces are a function of the local velocity in order to only reduce it and not to accelerate it in another direction. The forces are set at a defined distance upstream of the propeller and the distribution of them is calculated using an iterative process. First a computational mesh is constructed with the shaft and hub geometry but without propeller blades. This mesh is refined at the location for the forces and between this location and the propeller. The flow field is then computed and the axial flow velocities are compared to the desired axial wake and the force distribution up stream is set based on the differences found. However, the streamlines change shape and the water moves in other ways when a local flow resistance is applied. The flow field is, therefore recomputed and the resulting wake is analyzed. The force distribution is then adjusted, and the flow filed is again recomputed. This process is repeated until the force distribution converges and gives a sufficient representation of the wake.

3 COMPUTATIONAL EXAMPLES

3.1 Case 1

The first example focuses on two comparable designs with differences in the tip geometry, Figure 3.

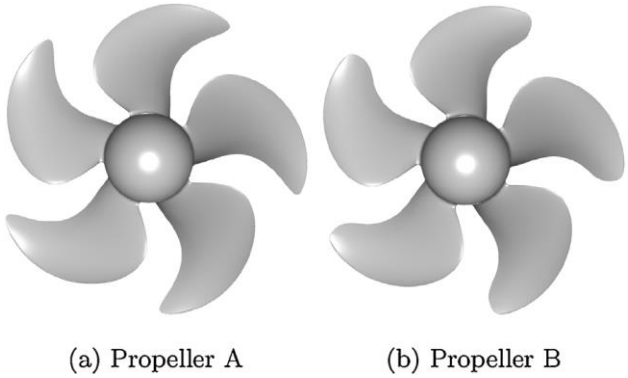

Figure 3: Propeller geometries.

Propeller A is a Kamewa standard high skew propeller with a low tip load. Propeller B is identical to propeller A except in the tip region, where a modification has been done to improve tip vortex cavitation inception; the sections close

to the tip of propeller B are shorter. This results in an even lower tip loading in propeller B compared to propeller A. To compensate for the reduced loading, the pitch is also increased slightly for propeller B to achieve thrust identity between the propellers at one chosen condition.

Both the cavitation tunnel experiments and the simulations were performed with a downstream shaft with 10 degrees inclination compared to the flow. This means that there were no axial wake, only a tangential wake. The cavitation bucket diagram from both the simulations and from cavitation tunnel tests can be found in Figure 4 and Figure 5 for propeller A and propeller B respectively. It can be seen in the figure that the method captures the lower inception sigma for propeller B compared to propeller A. However the shift in advance number, J, is not captured. Furthermore it can be seen that the simulation curves are a bit wavy which comes from the very simple inception criterion in combination with numerical noise. The numerical noise also contributes to that the inception occurs earlier in the simulation than in the experiment.

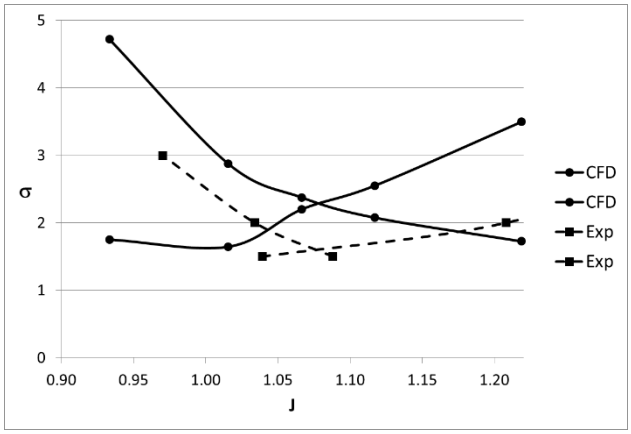

Figure 4: Cavitation bucket diagram for propeller A.

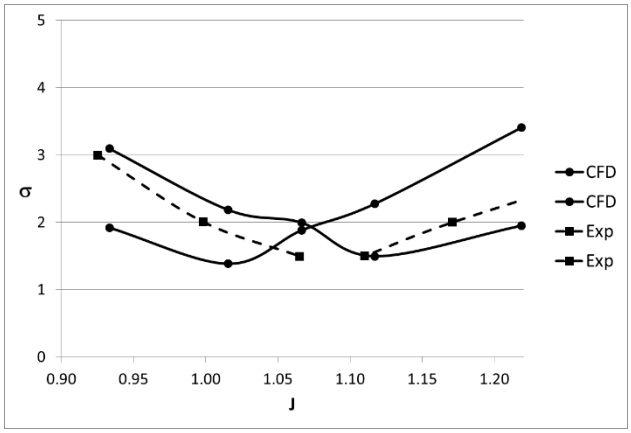

Figure 5: Cavitation bucket diagram for propeller B.

3.2 Case 2

The second example is one propeller mounted on the downstream end of an inclined shaft in a cavitation tunnel. The wake of the shaft is amplified by adding wire meshes onto the shaft casing upstream of the propeller; see Figure 6 and Figure 7. Two shaft angles, a1 = 7.5 and a2 = 11.5 degrees, and three meshes, in total 6 combinations, were tested. The coarsest mesh gave a wake similar to vessels with dual open shaft lines and the most dens mesh give a wake similar to single screw ships with a centre skeg.

Figure 6: Propeller, shaft and wake generating mesh inside the cavitation tunnel.

Figure 7: Three wake generating meshes with different density.

The bottom point of the cavitation bucket diagram, the point where the tip vortex domination switches side, was measured and calculated for all six combinations. The results are presented in Figure 8 and Figure 9 in two different ways. Figure 8 shows the advance number, J, and cavitation number, σ, for the six combinations by arrows starting at the CFD prediction, pointing at the EFD estimations. Here it can be seen that the difference between CFD and EFD is rather systematic for the two shaft angles and for mesh 2 and 3, capturing the trend of the changes in mesh density and shaft angle. Unfortunately there are larger deviations for mesh 1 which is the coarsest mesh corresponding to a small axial wake. More investigations are needed to find the reason for this deviation. However, a sharper wake gives a more defined inception point and reduces the uncertainty from other sources. The tip vortex starts normally on the blade when it enters into a pronounced wake but if the axial wake is weak compared to the tangential wake the tip vortex starts downstream of the blade which is harder both to predict and to find in a cavitation test. Differences in inception criteria in the

simulations and the experiments may be one explanation for the differences for the weak wake.

Figure 9 shows the same data as Figure 8 but normalized by experimental estimations. Here it can be seen that the estimation of the J value for the bottom of the bucket is within a few percent for mesh 2 and 3 while the deviation in σ is larger. It can also be seen that the σ value is under predicted for five of six combinations, which is a result of the over prediction of the pressure in the tip vortex and is something that can be fine-tuned by changing the volume criteria in the cavitation inception prediction. The absolute value is not critical for the method since it is intended to be used to compare different designs during the design process.

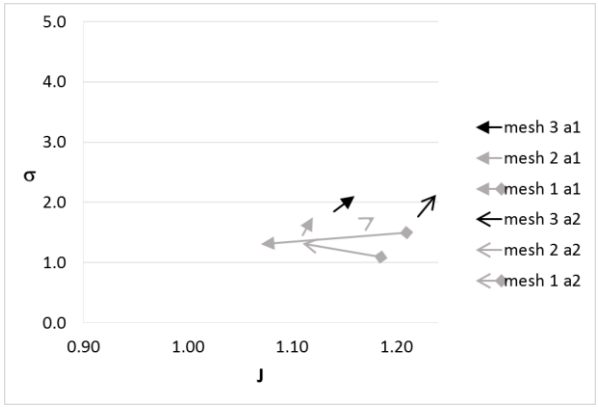

Figure 8: Calculated and measured bottom points for the cavitation bucket diagram, the arrows start at the CFD prediction and ends at the corresponding EFD estimation.

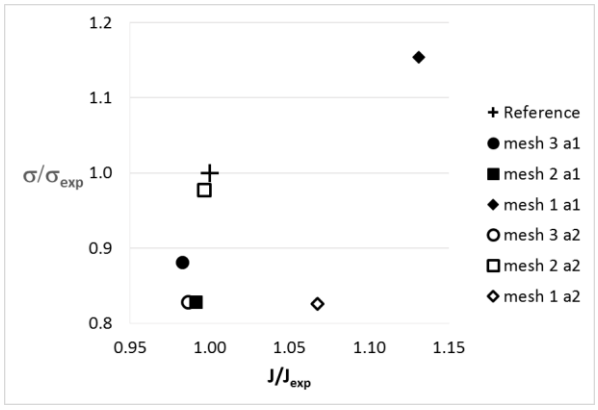

Figure 9: CFD prediction of bottom of the cavitation bucket normalized bye corresponding EFD estimations.

4 CONCLUSIONS

A method for tip vortex cavitation inception estimation at an industrial level has been presented. To make it feasible for industrial use in the propeller design process, which often has a relatively short timeframe, a compromise between accuracy and time consumption had to be done. The way to reduce the time consumption have been to have a lower mesh resolution than what is needed to fully accurate capture the development of the lowest pressure in the tip vortex. It is more important to capture the development of the tip vortex downstream of the blade if the tangential wake component is dominating over the axial wake component or if the axial wake component have a smooth distribution. It has also been shown that the condition, advance number, J, for the bottom of the cavitation bucket is captured accurately for conditions with moderate to strong wake but the inception cavitation number is not captured. However, the general trends are captured. This means that we have an engineering method which is not fully satisfactory from the scientific point of view. However, in an engineering context where the final propeller design is verified by model scale experiments, the uncertainty and over prediction of the pressure can be handled in an acceptable way. Furthermore, the systematic over prediction of the pressure becomes less problematic when the method primarily is used for comparison of different designs.

The method have been found useful by the propeller designers and have reduced the number of model tests needed to find a good design for challenging projects.

References

Arndt, R.E.A., Arakeri, V.H. and Higuchi, H., 1991: "Some observations of tip-vortex cavitation," Journal of Fluids Mechanics, 229: 269-289.

Asnaghi, A., Bensow, R.E., and Svennberg, U., 2017a: "COMPARATIVE ANALYSIS OF TIP VORTEX FLOW USING RANS AND LES," VII International Conference on Computational Methods in Marine Engineering, MARINE 2017At: Nantes, France.

Asnaghi, A., Bensow, R.E., and Svennberg, U., 2017b: "Implicit Large Eddy Simulation of Tip Vortex on an Elliptical Foil," Fifth International Symposium on Marine Propulsion, SMP'17At: Espoo, Finland.

Asnaghi, A., Svennberg, U., and Bensow, R.E., 2018a: "Numerical and experimental analysis of cavitation inception behaviour for high-skewed low-noise propellers," Applied Ocean Research, 79:197–214.

Asnaghi, A., Svennberg, U., and Bensow, R.E., 2018b: "Analysis of tip vortex inception prediction methods," Ocean Engineering, 167:187-203.

Hsiao, C.T. and Chahine, G., 2004: "Prediction of tip vortex cavitation inception using coupled spherical and nonspherical bubble models and Navier-Stokes computations," Journal of Marine Science and Technology, 8(3):99–108.

Hsiao, C.T. and Chahine G.L., 2005: "Scaling of Tip Vortex Cavitation Inception Noise With a Bubble Dynamics Model Accounting for Nuclei Size Distribution," Journal of Fluids Engineering," Vol. 127, page:55-65.

Kuiper, G., 1981: "Cavitation inception on ship propeller models," PhD-thesis Delft University of Technology.

Maines, B.H. and Arndt, R.E.A., 1997: "Tip vortex formation and cavitation. Journal of Fluids Engineering," Transactions of the ASME, 119(2):413–419.

Pennings, P., Westerweel, J. and Van Terwisga, T., 2015: "Sound signature of propeller tip vortex cavitation," Journal of Physics," 656(1).

Windt, J. and Bosschers, J., 2015: "Influence of local and adaptive mesh refinement on the tip vortex characteristics of a wing and propeller," In Computational Methods in Marine Engineering VI, pages 862–873.